**Supporting Information**

# Layered Xerogel Films Incorporating Monolayer Protected Cluster Networks on Platinum Black Modified Electrodes for Enhanced Sensitivity in First–Generation Uric Acid Biosensing

Mulugeta B. Wayu, Michael J. Pannell, Jonathan D. Dattelbaum, and Michael C. Leopold*
*Department of Chemistry, Gottwald Center for the Sciences, University of Richmond*
*Richmond, VA 23173*

**CONTENTS:**



* To whom correspondence should be addressed. Email: mleopold@richmond.edu. Phone: (804) 287–6329. Fax: (804) 287–1897

**Uricase Enzyme Synthesis Details**

Urate oxidase or uricase (UOx) enzyme from *Bacillus fastidiosus* (~9 U/mg) and *Candida sp.* (≥ 2U/mg) were purchased from Sigma Aldrich. Additionally, *Bacillus fastidiosus* (ATCC strain 29604) UOx gene was obtained from the NCBI database and synthesized by GenScript (Piscataway, NJ) cloned into the NdeI/XhoI site of the pET-21a expression vector. The gene was codon-optimized for expression in an *Escherichia coli* background prior to synthesis using the optimization tool constructed by Integrated DNA Technologies (Coralville, IA). Plasmids were transformed into chemically competent Rosetta–gami (DE3) cells and were selected on LB agar plates containing ampicillin (100 μg $mL^{-1}$). Single colonies were incubated overnight at 37 ˚C while shaking in 2xYT broth containing ampicillin (100 μg $mL^{-1}$). Fresh media was inoculated 1:40 for overexpression at 37 ˚C. Mid–log phase cells were induced with IPTG (0.2 mM) for 3–4 hrs. The cells were collected by centrifugation (4,000 rpm, 10 min.) and resuspended in 30 mL lysis buffer (50 mM phosphate, pH 8.0, 200 mM NaCl, and 10 mM imidazole). The cells were then lysed by sonication, and the cell debris was removed by centrifugation (13,000 rpm, 25 min). The supernatant was added to a Ni–NTA column for purification by affinity chromatography. UOx was bound to the column via a C–terminal 6xHis tag and was extensively washed with 20 mM imidizole prior to elution with 250 mM imidizole. At this point, the protein was buffer exchanged into 5 mM phosphate, pH 7.0 and lyophilized (Labconco) overnight for long–term storage at –20˚C.

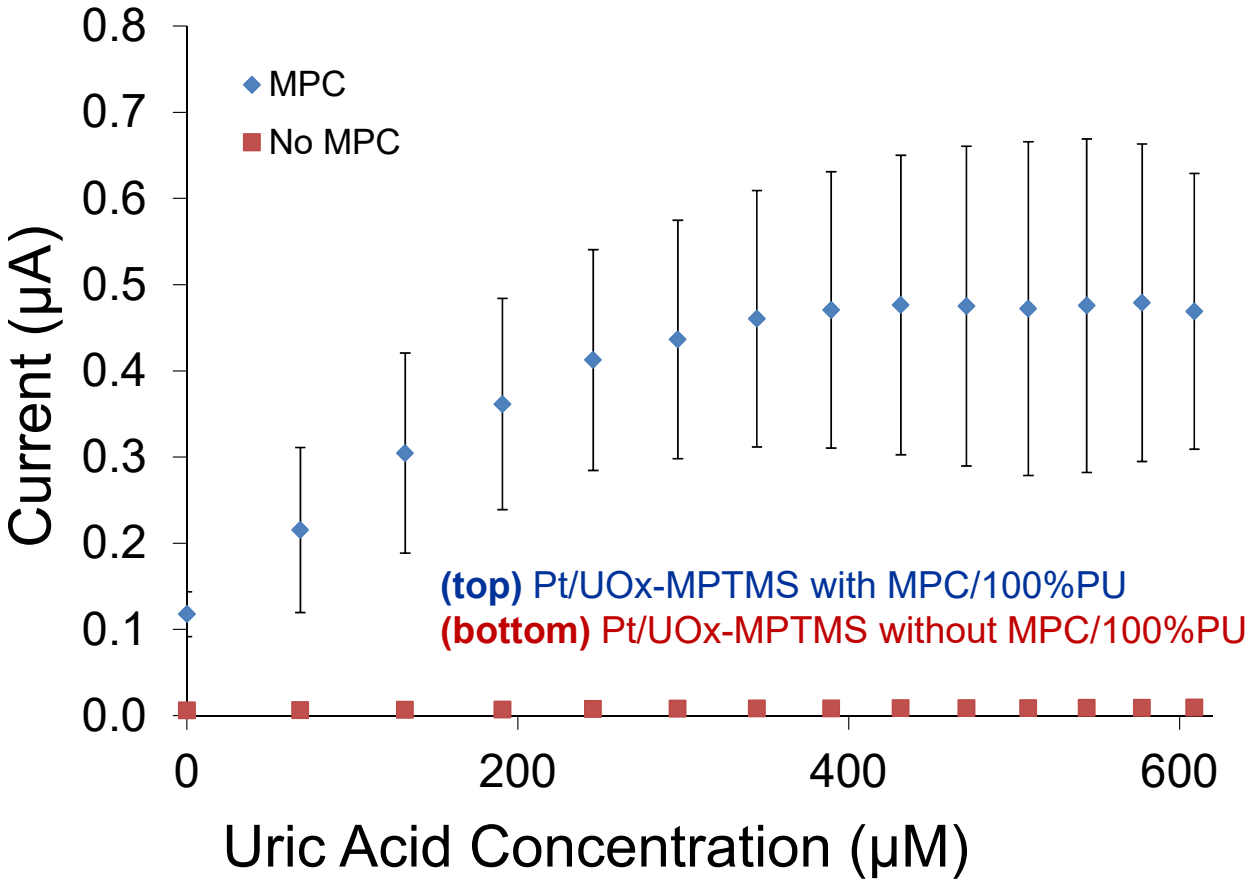


**Figure SI-1.** Preliminary calibration curve results for platinum electrodes modified with MPTMS xerogels with (n=11) and without (n=10) MPC doping and capped with polyurethane layers (100%HPU). Note: In some cases, error bars are smaller than markers for average. These films do not have the diffusional xerogel layer or the electropolymerized semi-permeable membrane (n=4).

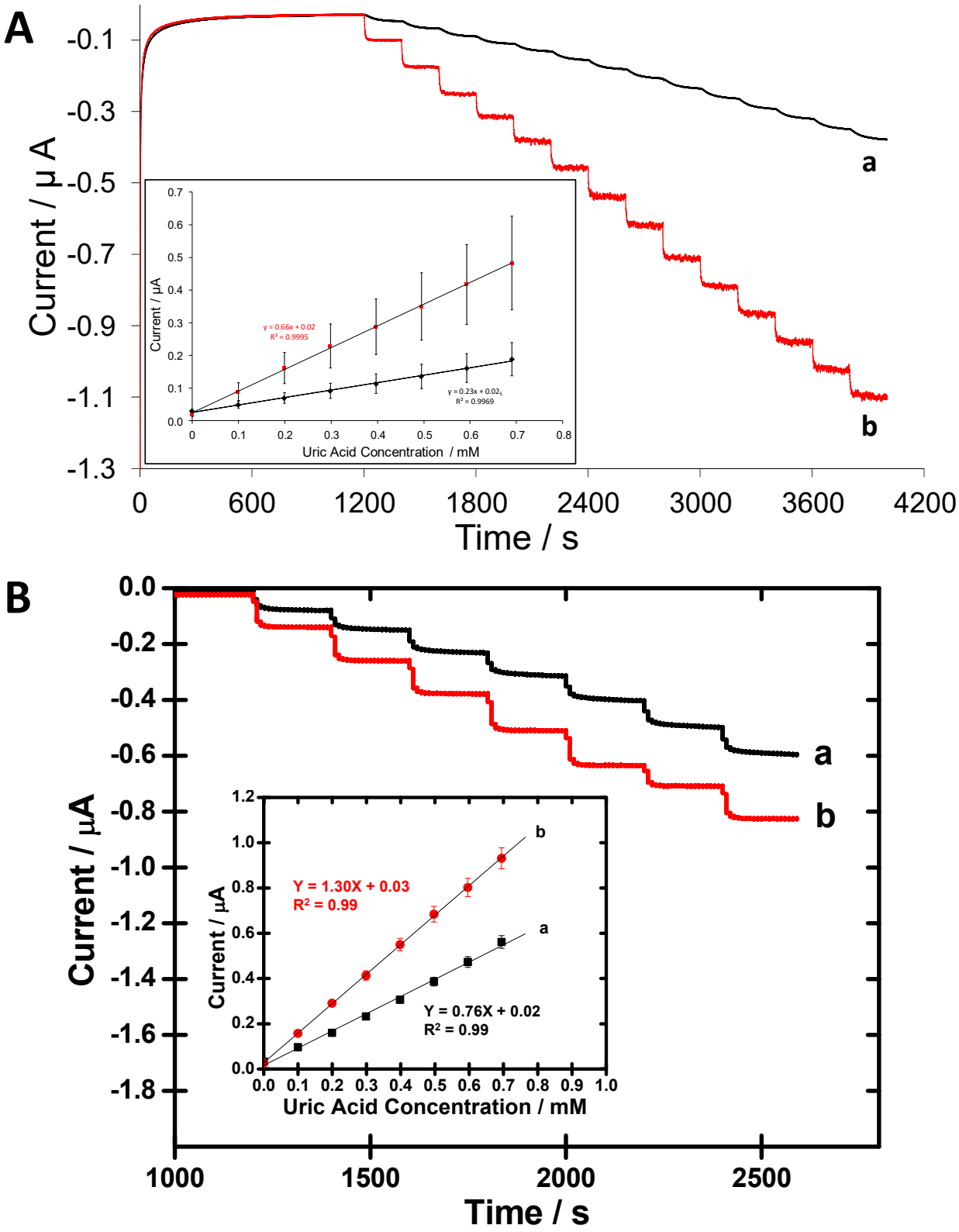


**Figure SI-2.** Initial **(A)** (n=3) and additional example **(B)** (n=5) of amperometric i-t curves and corresponding calibration curves **(inset)** during successive 0.1 mM injections of UA at a Pt electrode modified with UOx-doped HMTES xerogel **(a)** without or **(b)** with MPC incorporation, undoped HMTES xerogel, and PU layer (100% HPU). Note: In some cases, error bars are smaller than markers for average (n=-3).

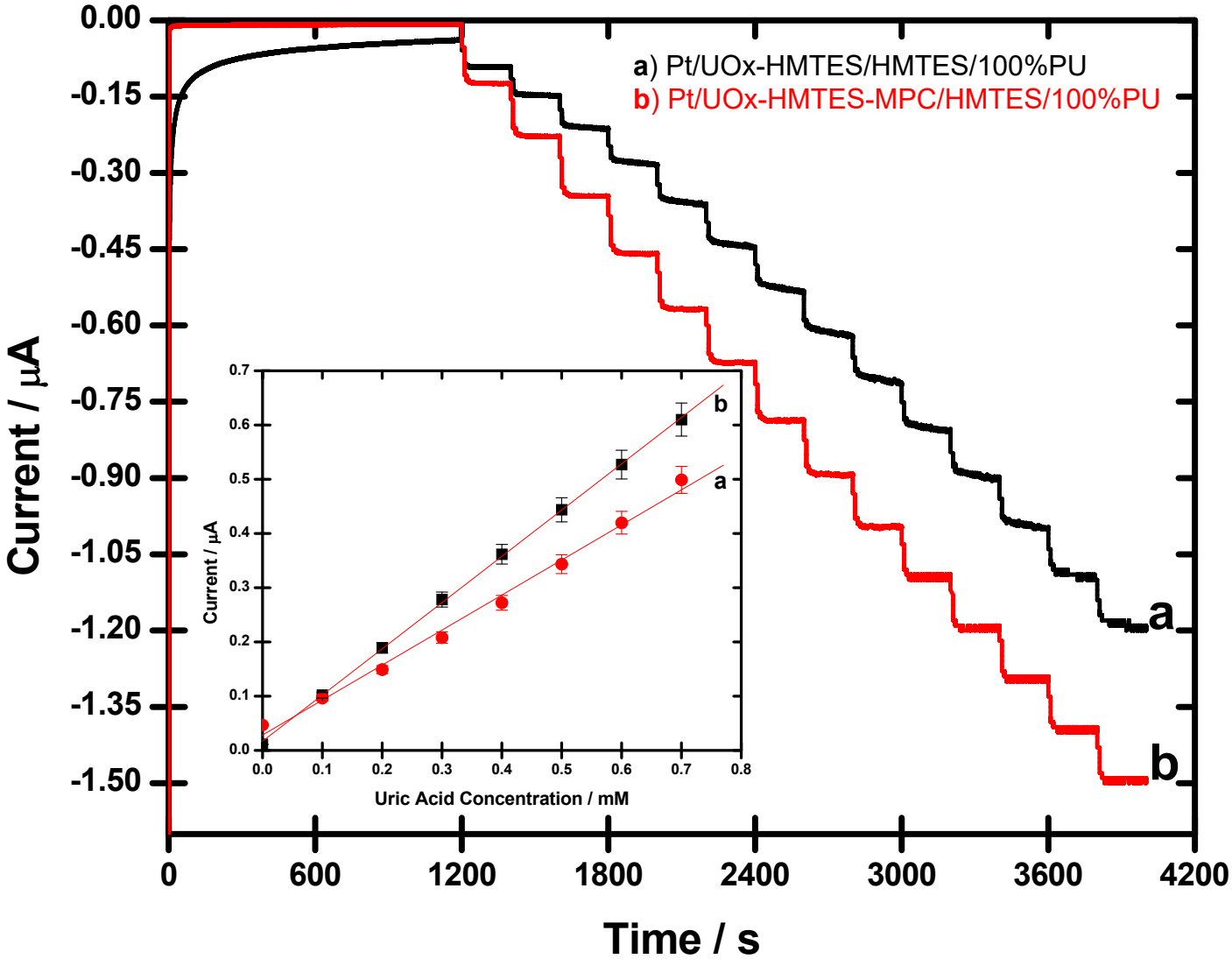


**Figure SI-3.** Amperometric i-t curves and corresponding calibration curves **(inset)** during successive 0.1 mM injections of UA at a Pt electrode modified with UOx-doped HMTES xerogel **(a)** without or **(b)** with MPC incorporation, undoped HMTES xerogel, and PU layer (100% HPU). Note: In some cases, error bars are smaller than markers for average (n = 3).

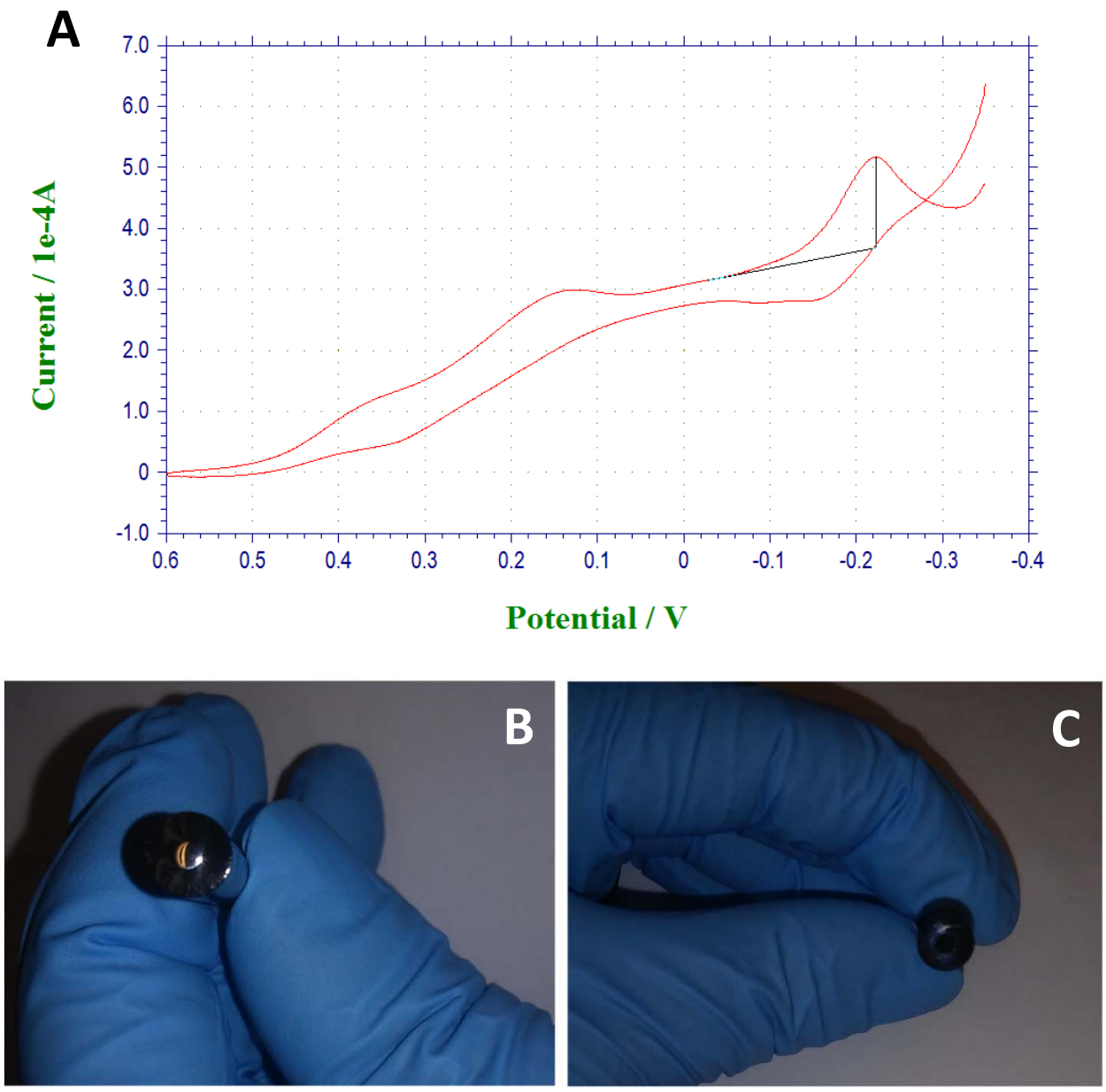


**Figure SI-4.** **(A)** Cyclic voltammetry during platinization to form platinum black at a clean platinum electrode; solution is 3% chloroplatinic acid (v/v in water) by cycling the potential from +0.6 to −0.35 V (vs Ag/AgCl) at sweep rate of 20 mV/s; **(B, C)** Photographs of platinum electrode before and after application of platinum black modification.

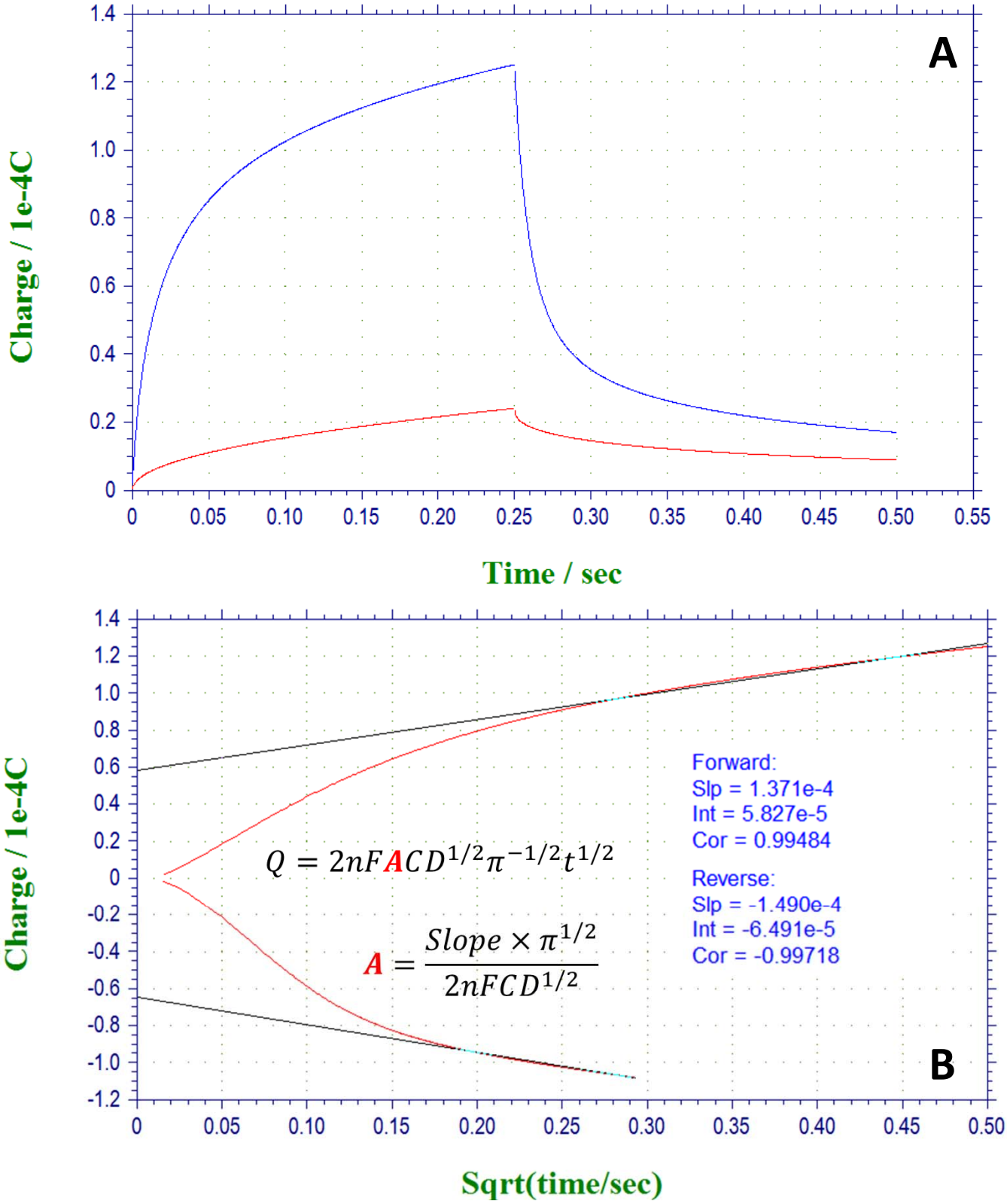


**Figure SI-5. (A)** Charge vs. time plot for chronocoulometry experiments of 5mM $K_3Fe(CN)_6$ (0.5 M KCl) where the potential is stepped from a potential with negligible Faradaic current (X V) to +0.60 V (vs. Ag/AgCl) for **(a)** and **(b)** ; **(B)** Corresponding Anson plot (charge vs. time$^{1/2}$) to determine the area of the electrode (inset equations).

**Table SI-1.** Chronocoulometry (CC) and Cyclic Voltammetry (CV) Summary for Cathodic Waves of 5 mM Potassium Ferricyanide (0.5 M KCl) After Platinization of Platinum Electrodes.

| Pt–B Layers | Average Area ($cm^2$) from CC | CV Average $I_{p,c}$ (µA) [a] | CV Average $I_{p,c}$ (µA) [b] | CV Average $I_{p,c - BG}$ (µA) [c] | DPV Average $I_{p,c}$ (µA) [d] |
|---|---|---|---|---|---|
| 0 | 0.03 ±0.01 | 35.50 ±1.34 | 30.35 ±0.17 | 32.20 ±0.24 | 38.65 ±0.54 |
| 1 | 0.07±0.01 | 49.76 ±0.29 | 27.26 ±0.70 | 31.33 ±1.04 | 56.51 ±0.1 |
| 2 | 0.09 ±0.02 | 67.14 ±1.34 | 26.12 ±0.59 | 32.30 ±1.67 | 59.71 ±1.21 |
| 3 | 0.14 ±0.03 | 83.67 ±1.92 | 25.86 ±0.46 | 34.39 ±1.34 | 60.54 ±0.62 |
| 4 | 0.18 ±0.04 | 101.43 ±1.53 | 24.26±0.46 | 38.60 ±1.27 | 61.07 ±0.13 |

**Notes:** - Uncertainty values listed represent standard deviation (n=4).

[a] Faradaic and non-Faradaic (charging) peak current ($i_{p,c}$).

[b] Isolated Faradaic current from individual peak analysis.

[c] Isolated Faradaic current after background subtraction of same scans in 0.5 M KCl supporting electrolyte.

[d] Isolated Faradaic current from individual peak analysis;
**DPV parameters:** Potential window = 0↔+0.4 V; Pulse width = 0.05 s; Amplitude = 0.05 V; Period = 0.5 s; Sensitivity 1E-4 A/V

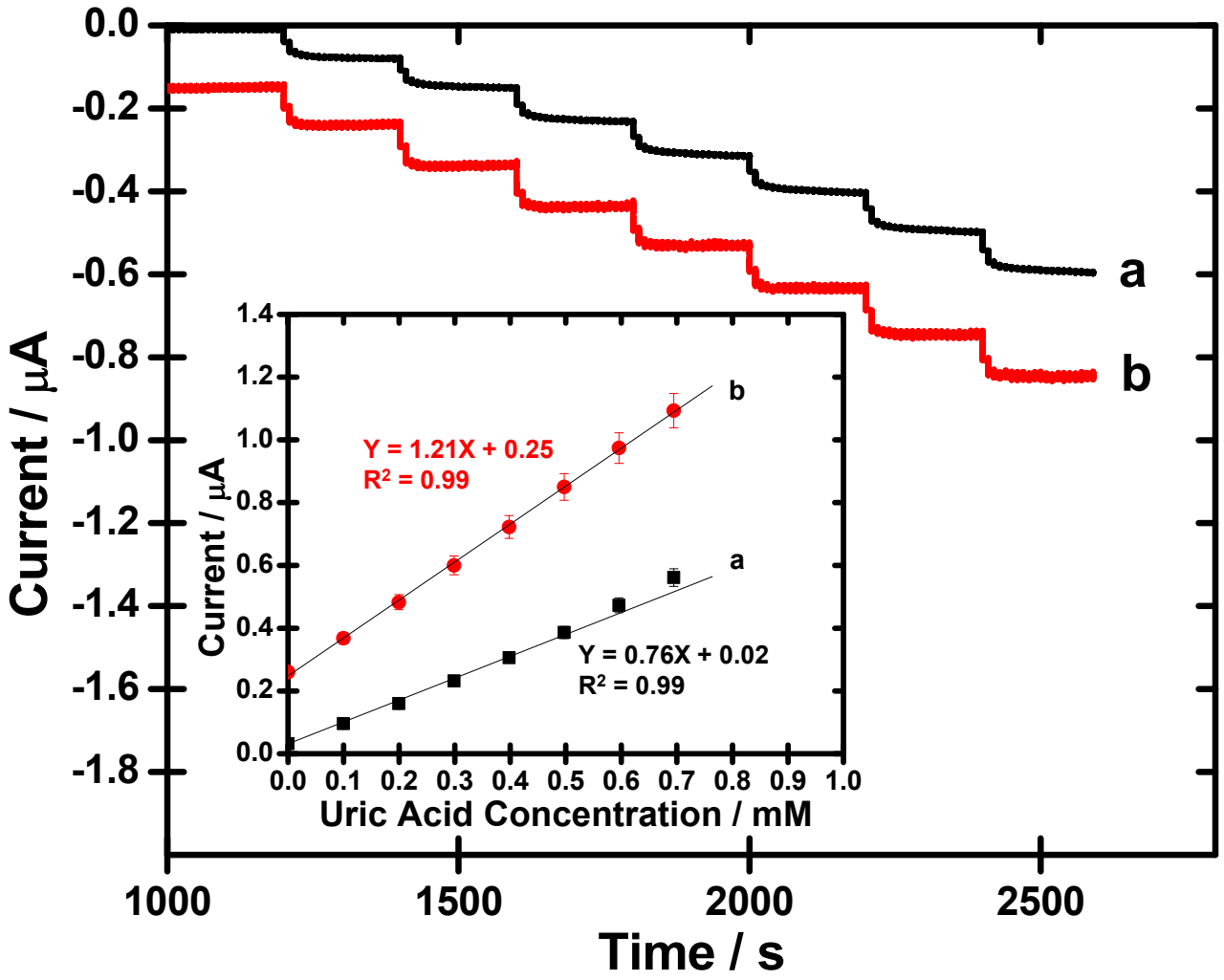


**Figure SI-6.** Additional example of representative amperometric I–t curves and corresponding calibration curves (**Inset**) during successive 0.1 mM injections of uric acid at platinum electrodes modified with (**a**) UOx embedded HMTES xerogel and (**b**) Pt–B and UOx embedded HMTES xerogel, each coated with undoped xerogel followed by HPU. Notes: In some cases, standard error bars are smaller than markers for average value (n = 4).

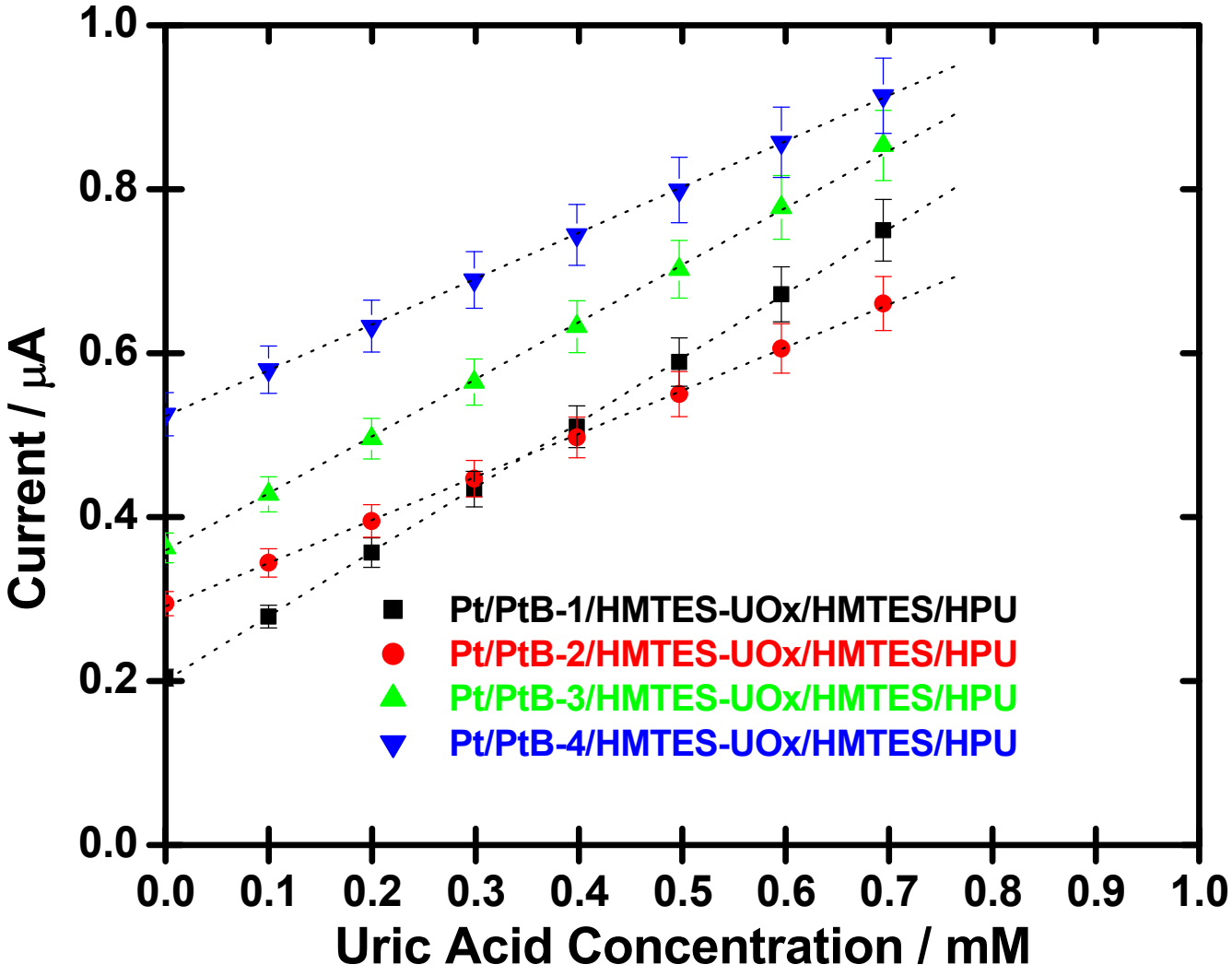


**Figure SI-7.** (**A**) Representative calibration curves during successive 0.1 mM injections of uric acid at platinum electrodes modified with Pt–B (1 → 4 layers) and UOx embedded HMTES xerogel, followed by undoped HMTES xerogel and capped with PU (100% HPU). Pt – B layers – 1 and 3 seem to yield higher sensitivity whereas Pt–B layers of 2 and 4 showed a slight decrease in sensitivity. Note: In some cases, standard error bars are smaller than markers for average value (n=4).

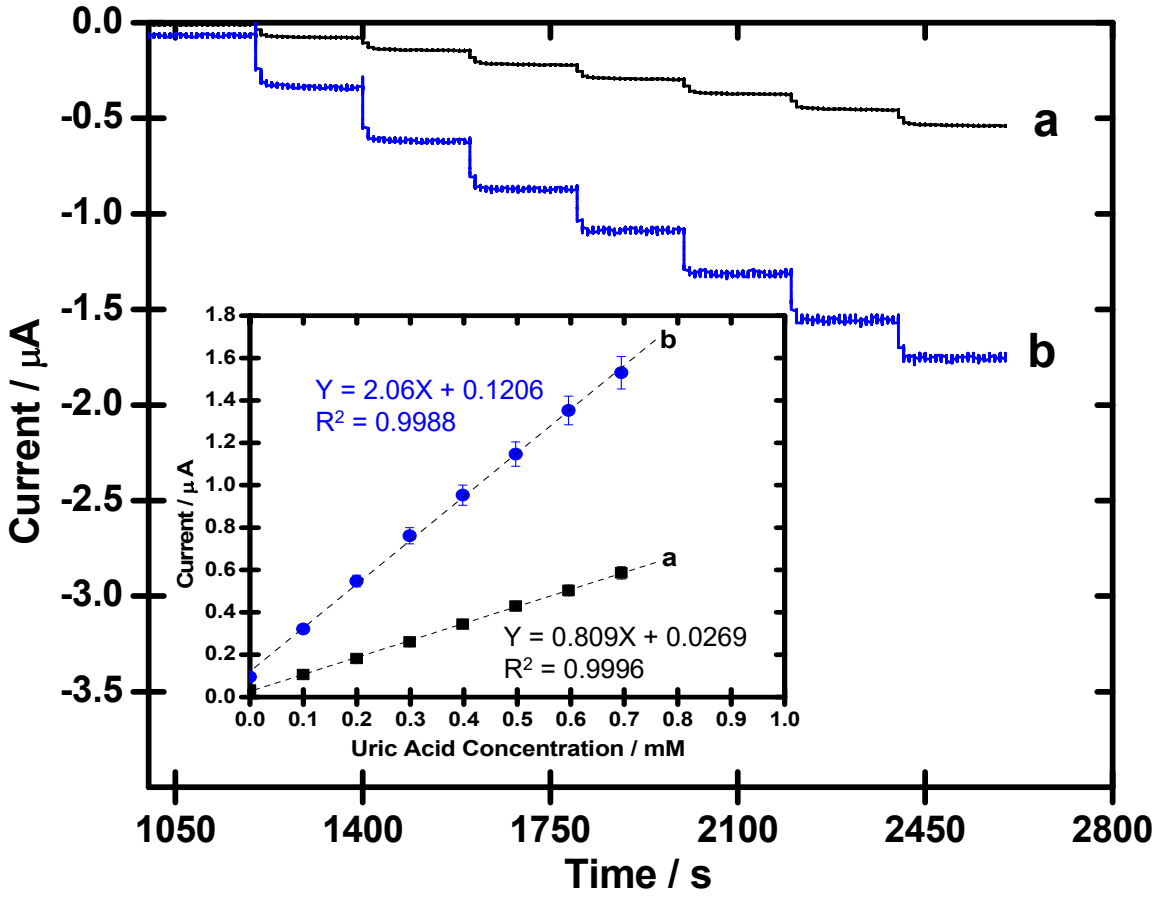


**Figure SI-8.** Amperometric i-t curves and corresponding calibration curves **(inset)** during successive 0.1 mM injections of UA at a **(a)** Pt electrode modified with HMTES xerogel with UOx or **(b)** a Pt-B modified electrode with MPC-doped HMTES xerogel with UOx and each having undoped HMTES xerogel and PU layer (100% HPU) capping layers. Note: In some cases, error bars are smaller than markers for average (n =4).

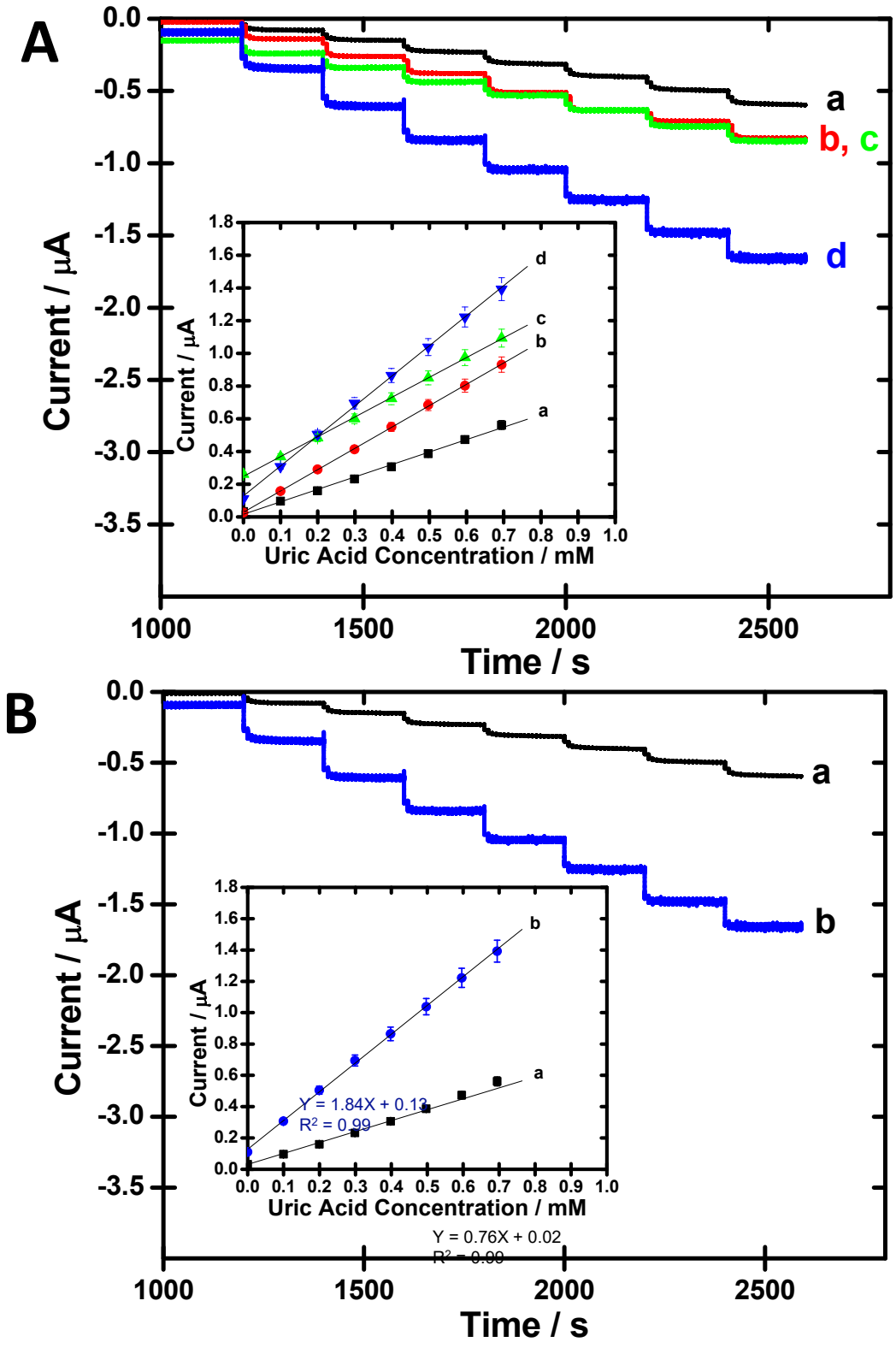


**Figure SI-9. (A)** Representative amperometric i-t curves and corresponding calibration curves (**Inset**) during successive 0.1 mM injections of uric acid at platinum electrodes modified with (**a**) UOx embedded HMTES xerogel, (**b**) UOx embedded HMTES xerogel doped with MPCs, (**c**) Pt–B and UOx embedded HMTES xerogel, and (**d**) Pt–B and UOx embedded HMTES xerogel doped with MPCs, each coated with undoped xerogel followed by HPU; **(B)** A direct comparsion between **(a)** UOx embedded HMTES xerogel and **(b)** ) Pt–B and UOx embedded HMTES xerogel doped with MPCs, each coated with undoped xerogel followed by HPU (curves (a) and (d) from part A). Note: In some cases, standard error bars are smaller than markers for average value (n=3-4).

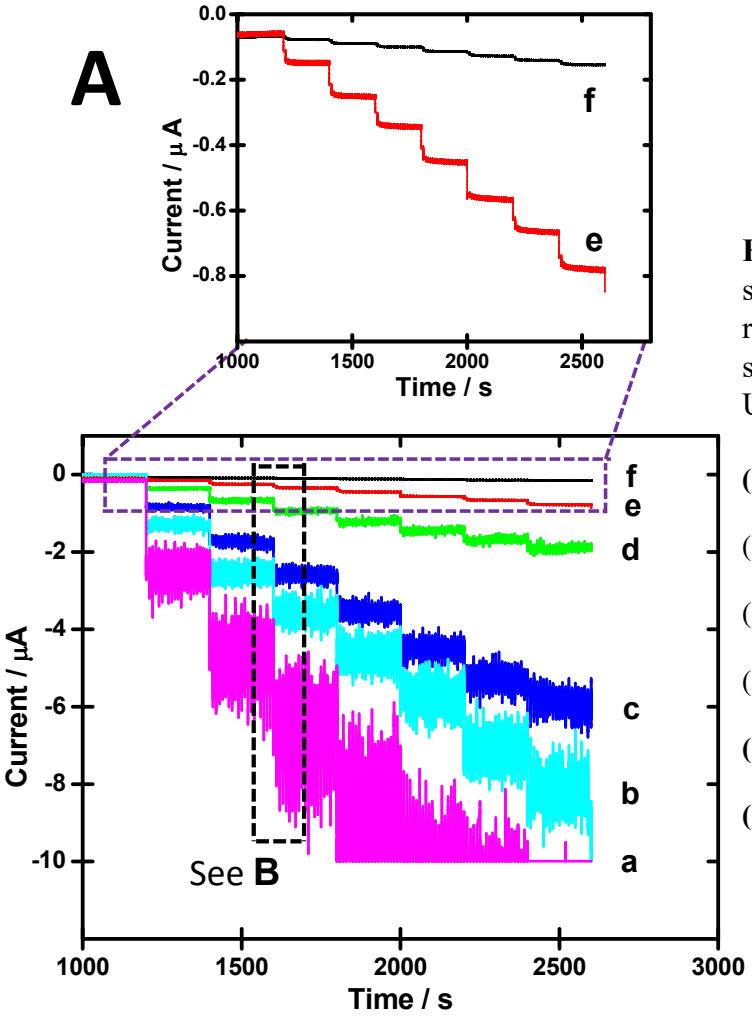


**Figure SI-10. (A)** Amperometric i-t curves during successive injections of UA and **(B)** current response comparison as a function of layering system for third UA injection (i.e., 3rd step, ~300 μM UA) at the following films:

**(a)** Pt/Pt-B;

(**b**) Pt (bare);

(**c**) Pt/UOx-HMTES-MPC/HMTES;

(**d**) Pt/UOx-HMTES-MPC/HMTES/PL-A;

**(e)** Pt/Pt-B/UOx-HMTES-MPC/HMTES/PL-A/100%HPU;

**(f)** Pt/UOx-HMTES-MPC/HMTES/PL-A/ 100%HPU

Note: Error bars in Figure SI-8B represent standard error (n = 3).

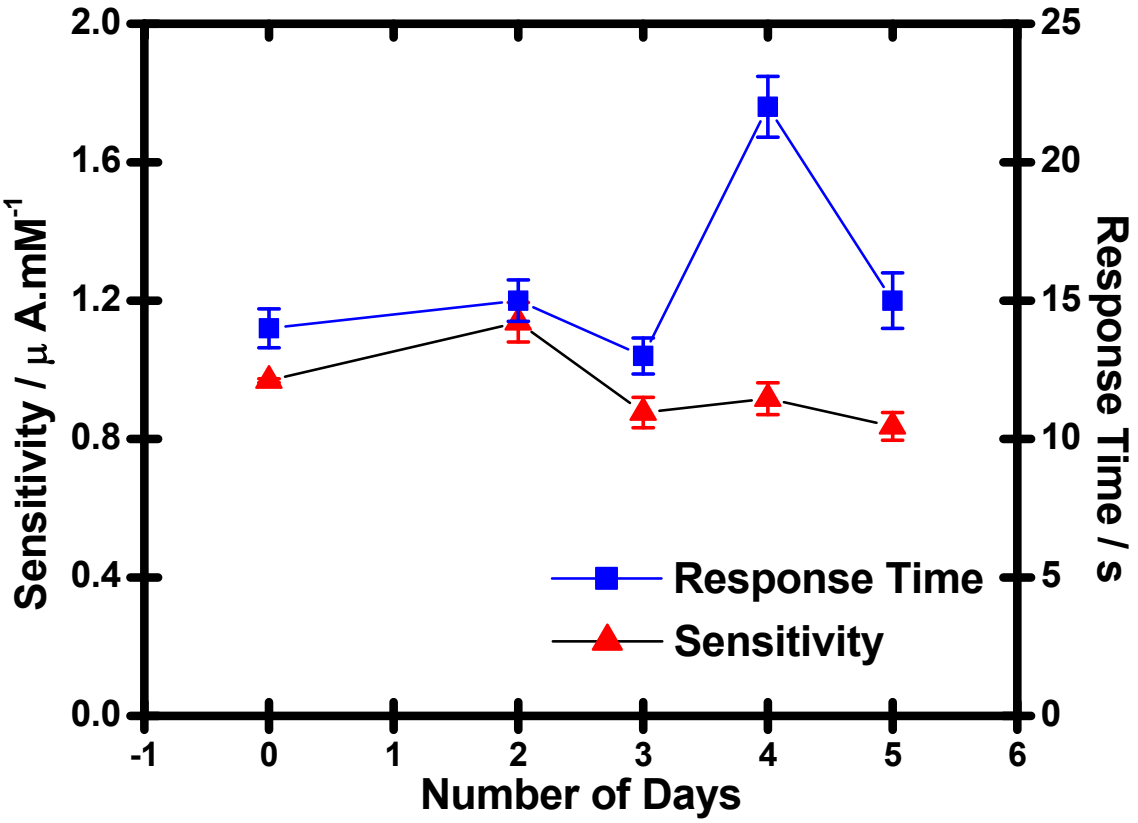


**Figure SI-11.** Sensitivity and response time ($t_{R\text{-}95\%}$) of Pt/Pt-B/UOx-HMTES-MPC/HMTES/PL-A/100%HPU UA biosensor over a period of 5 days. Note: In some cases, standard error bars are smaller than markers for average value (n = 4).

**Table SI-2.** Selectivity Coefficient Comparison from Glucose Biosensing Literature†

| Interferent Species | Reference 2a (Glucose) | Reference 2a (Glucose) w/ MPCs | Reference 8 (Glucose) | Reference 10 (Glucose) | Reference 20 (Glucose) | This Work (Uric Acid) |
|---|---|---|---|---|---|---|
| Acetaminophen (100 μM) | 0.89 (±0.14) | 0.64 (±0.20) | -1.146 (±0.2847) | -- | 0.96 | 0.14 (±0.13) |
| Ascorbic Acid (100 μM) | 0.39 (±0.15) | -0.47 (±0.15) | -2.265 (±0.663) | -- | -0.73 | -1.11 (±0.22) |
| Sodium Nitrite (100 μM) | 0.04 (±0.44) | NR | -1.943 (±0.458) | -1.90 ($^{-}$2.00 - $^{-}$3.21) | -- | 0.04 (±0.09) |
| Oxalic Acid (100μM) | NR | NR | -1.974 (±0.145) | -- | -- | -1.08 (±0.16) |
| Glucose (3.0 mM) | -- | -- | 0.1617 (±0.1408) | -- | -- | -1.65 (±0.52) |
| Uric Acid (300 μM) | NR | NR | -1.168 (±0.129) | -- | 0.28 | 0.16 (±0.03) |

**Notes:** †Referenced work varies in type of silane xerogel as well as normalization concentration in determining individual selectivity coefficients (denominator of general form equations[8,10,18] below for glucose and uric acid biosensor systems):

$$K_{Glucose,\ j}^{amp} = \log\left(\frac{\Delta I_j / C_j}{\Delta I_{Glucose} / C_{Glucose}}\right)$$

$$K_{UA,\,j}^{amp} = \log\left(\frac{\Delta I_j / C_j}{\Delta I_{UA} / C_{UA}}\right)$$

where $\Delta I_j$ and $\Delta I_{glucose}$ are the measured currents for a specific interferent species (j) and glucose at concentrations of $C_j$ and $C_{glucose}$, respectively (or interferent species (j) and uric acid at concentrations of $C_j$ and $C_{uric\ acid}$ interferent species, respectively).

Refs. 10, 18 normalize to 5.6 mM glucose whereas Refs. 2 and 8 use 1 mM as their standard; the current UA biosensing scheme uses 300 μM, a conservative approach to selectivity coefficients.